



# Computer simulation of topological defects around a colloidal particle or droplet dispersed in a nematic host

DENIS ANDRIENKO, MICHAEL P. ALLEN, AND GUIDO GERMANO<sup>1</sup>

H. H. Wills Physics Laboratory, University of Bristol, Tyndall Avenue, Bristol BS8 1TL, United Kingdom

<sup>1</sup>Fakultät für Physik, Universität Bielefeld, 33501 Bielefeld, Germany

## Abstract

We use molecular dynamics to study the ordering of a nematic liquid crystal around a spherical particle or droplet. Homeotropic boundary conditions and strong anchoring create a hedgehog director configuration on the particle surface and in its vicinity; this topological defect is cancelled by nearby defect structures in the surrounding liquid crystal, so as to give a uniform director field at large distances. We observe three defect structures for different particle sizes: a quadrupolar one with a ring defect surrounding the particle in the equatorial plane; a dipolar one with a satellite defect at the north or south pole; and a transitional, non-equatorial, ring defect. These observations are broadly consistent with the predictions of the simplest elastic theory. By studying density and order-parameter maps, we are able to examine behaviour near the particle surface, and in the disclination core region, where the elastic theory is inapplicable. Despite the relatively small scale of the inhomogeneities in our systems, the simple theory gives reasonably accurate predictions of the variation of defect position with particle size.

## Saturn ring

For all studied radii ( $R/\sigma_0 = 3-15$ ) the ring defect appears immediately after equilibration of the system starting from the isotropic state or blowing up the droplet in the nematic state. We therefore concluded that this type of the defect is energetically more favourable for the chosen droplet sizes.

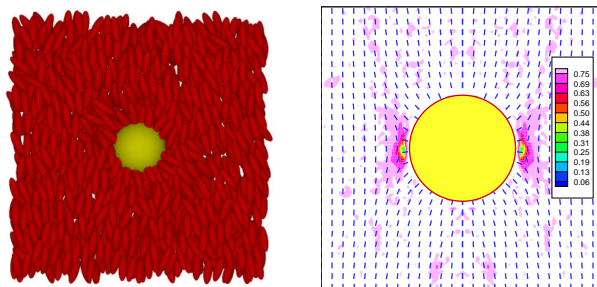


Figure 2,3 Configuration slice and the director profile of the ring defect.

A typical slice and a director map of the ring defect obtained from the simulations is shown in Figs. 2,3. From this map one can see that the ring defect does not have long-range director distortions. Its core region is located very close to the droplet surface and the director distortion vanishes very quickly in the liquid crystal bulk. This is in agreement with the quadrupolar nature of the defect: far from the particle the director deviation angle has asymptotic behaviour  $\beta \sim (R/r)^3 \sin 2\theta$ .

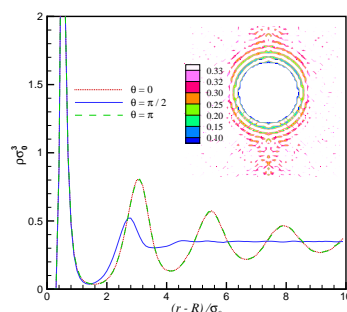


Figure 4 Density profiles for the ring defect. Droplet radius  $R/\sigma_0 = 15$ . The following directions are shown:  $\theta = 0, \pi$  (avoiding the defect) and  $\theta = \pi/2$  (crossing the disclination ring). The inset shows the contour plot of the density map.

Typical density profiles for the ring defect with  $R = 15$  are shown in Fig. 4 for  $\theta = 0, \pi$  (not intersecting the defect) and  $\theta = \pi/2$  (crossing the disclination ring). The profiles which avoid the disclination have oscillating structure near the particle surface which is typical for a liquid-wall interface. The profiles which cross the disclination ring do not have oscillations. The difference may be due to the partial melting of the liquid crystal in the disclination core region. This melting damps the influence of the droplet surface on the interface.

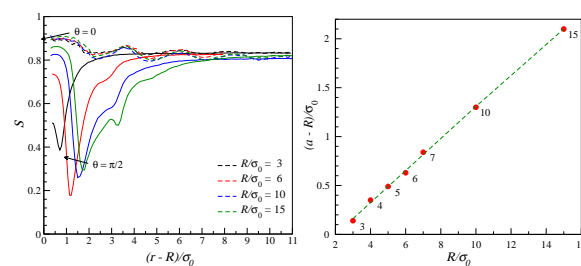


Figure 5 Order parameter profiles for the ring defect along the directions  $\theta = 0, \pi/2$ . Different curves correspond to the different droplet radii.

Figure 6 Distance of the core region of the ring defect from the droplet center, as a function of reduced droplet radius  $R/\sigma_0$ . We also show the linear fit to the simulation results,  $a_r = 1.164R - 0.33\sigma_0$ .

The order parameter profiles for  $\theta = 0, \pi/2$  are shown in Fig. 5. The shape of these profiles in general reflects the typical structure of the core: the center of the core has lower order than the bulk and the core region extends over a few molecular lengths. Using the minima of the order profiles we extracted the distance from the core of the disclination ring to the particle surface. The dependence of this distance on the particle radius  $R$  is shown in Fig. 6. It is interesting to compare with the phenomenological theory predicting linear dependence of the ring defect radius on the droplet radius:  $a_r \approx 1.25R$  from minimization of the elastic free energy using a trial function [3],  $a_r \approx 1.13R$  using a simulated annealing method [4], or  $a_r \approx 1.26R$  [5]. Our MD simulation results give  $a_r - R = -0.33\sigma_0 + (0.164 \pm 0.004)R$  which is in good agreement with the phenomenological theory, especially if one bears in mind the complex structure of the defect core.

## Satellite defect

The director field around the satellite defect is illustrated in Fig. 8. The director distortion extends much further than that of the ring defect. This is a direct consequence of the symmetry of the director distribution of the satellite defect: far from the particle, the director angle vanishes as  $\beta \sim (R/r)^2 \sin \theta$ , i.e. it is like a dipolar term in a multipole expansion.

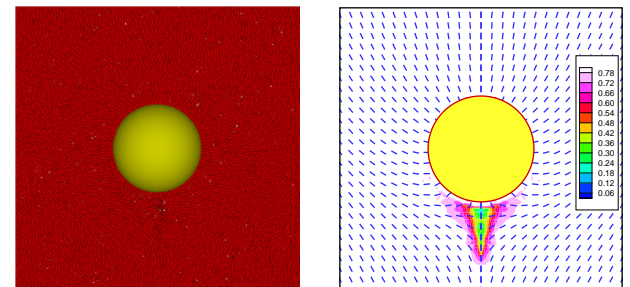


Figure 7,8 Configuration slice and the director profile of the Satellite defect. Droplet radius  $R/\sigma_0 = 15$ . The background contour plot represents the value of the order parameter.

To study the satellite defect, one needs very large systems. We used one million particles and droplet radius  $R = 15$ . The density profiles for the satellite defect are shown in Fig. 9. One can see that the density profile at  $\theta = \pi$  (across the defect core) has less prominent oscillating structure than the other two: this is again presumably due to the partial disordering of the mesophase in the core region.

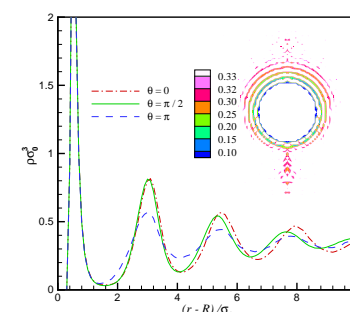


Figure 9 Density profiles for the satellite defect. Droplet radius  $R/\sigma_0 = 15$ . The following directions are shown:  $\theta = 0, \pi/2$  (both avoiding the defect) and  $\theta = \pi$  (crossing the defect). The contour plot of the density map is shown in the inset.

The center of the defect core is located at a distance  $a_s \approx 1.4R$ . The value predicted by the elastic theory is about  $1.22R$  for the simulated annealing calculations [4];  $1.17R$  [1] or  $1.46R$  [7] for the free energy minimization using a trial function.

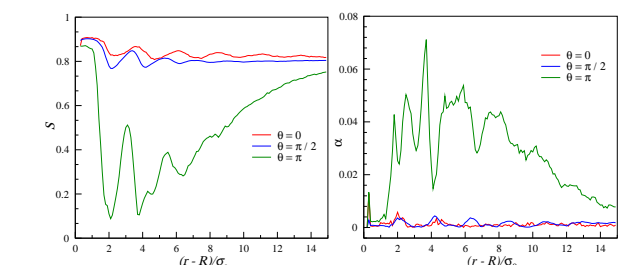


Figure 10 Order parameter profiles for the satellite defect along the directions  $\theta = 0, \pi/2, \pi$ .

Figure 11 Biaxiality profiles for the satellite defect ( $\theta = 0, \pi/2, \pi$ ). Droplet radius  $R = 15$ .

## Introduction

Suspensions of solid particles or immiscible liquid droplets in a host fluid (colloids) have attracted wide interest, due to a number of industrial applications (they appear in food, paints, ink, drugs) and fundamental research (they show features such as Casimir forces between the particles, formation of supermolecular structures and novel phases). Colloidal systems with a liquid crystal as a host fluid are of special interest [1].

Elastic deformations of the director field around the colloidal particles produce additional long-range forces between them. These interactions can be of dipolar or quadrupolar type depending on the symmetry of the director field around the particles [2], and this in turn is extremely sensitive to the boundary conditions on the particle surface and the size of the particles [3].

The complication here is the presence of topological defects in such emulsions. Isolated drops provide a spherical confining geometry for the liquid crystal. Sufficiently strong homeotropic anchoring of the director (that is, normal to the particle surface) then induces a radial hedgehog defect with topological charge  $+1$ . If the director field is uniform far from the particle, i.e. the total charge of the whole system is zero, topological considerations imply that an additional defect must be created in the medium to compensate the radial hedgehog.

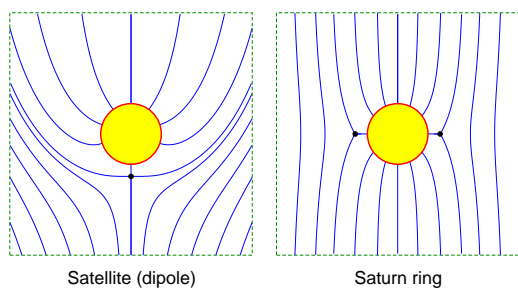


Figure 1 Sketches of the satellite defect and Saturn ring defect.

There are several types of defect which can arise in this case. Two are illustrated in Fig. 1. The first is a hyperbolic hedgehog with a topological charge  $-1$ , called a dipolar or satellite defect. The second is a quadrupolar or Saturn-ring defect, i.e. a  $-1/2$  strength disclination ring that encircles the spherical particle. Theoretical and numerical work based on the elastic theory [4, 5] suggest that the dipole configuration is stable for the micron-sized droplets which are usually realised experimentally; the Saturn-ring configuration should appear if the droplet size is reduced and, when present, it is always predicted to be most stable in the equatorial plane normal to the director.

## Molecular model and simulation methods

Molecular dynamics simulations were carried out using axially symmetric molecules interacting through the pair potential

$$v_{ij} = \begin{cases} 4\epsilon_0 (\varrho_{ij}^{-12} - \varrho_{ij}^{-6}) + \epsilon_0, & \varrho_{ij}^6 < 2 \\ 0, & \varrho_{ij}^6 > 2 \end{cases} \quad (1)$$

Here  $\varrho_{ij} = (r_{ij} - \sigma_{ij} + \sigma_0)/\sigma_0$ ;  $r_{ij}$  is the center-center separation,  $\sigma_0$  a size parameter,  $\epsilon_0$  an energy parameter (both taken to be unity) and the orientation-dependent diameter  $\sigma_{ij}$  is defined by

$$\sigma_{ij} = \sigma_0 \left\{ 1 - \frac{\chi}{2} \left[ \frac{(\hat{\mathbf{r}}_{ij} \cdot \hat{\mathbf{u}}_i + \hat{\mathbf{r}}_{ij} \cdot \hat{\mathbf{u}}_j)^2}{1 + \chi(\hat{\mathbf{u}}_i \cdot \hat{\mathbf{u}}_j)} + \frac{(\hat{\mathbf{r}}_{ij} \cdot \hat{\mathbf{u}}_i - \hat{\mathbf{r}}_{ij} \cdot \hat{\mathbf{u}}_j)^2}{1 - \chi(\hat{\mathbf{u}}_i \cdot \hat{\mathbf{u}}_j)} \right] \right\}^{-1/2}$$

where  $\chi = (\kappa^2 - 1)/(\kappa^2 + 1)$ ,  $\kappa$  being the elongation. In this work we used  $\kappa = 3$  throughout. The orientation dependence is written in terms of the direction of the center-center vector  $\hat{\mathbf{r}}_{ij} = \mathbf{r}_{ij}/r_{ij}$  and the unit vectors  $\hat{\mathbf{u}}_i, \hat{\mathbf{u}}_j$  which specify the molecular symmetry axes. This is a soft repulsive potential, describing (approximately) ellipsoidal molecules; it may be thought of as a variant of the standard Gay-Berne potential [6] with exponents  $\mu = 0, \nu = 0$ . The molecular mass  $m$  was taken to be unity, and the molecular moment of inertia fixed as  $I = 2.5m\sigma_0^2$ .

The interaction of molecule  $i$  with the droplet was given by a shifted Lennard-Jones repulsion potential between the centers, having exactly the same form as eqn (1), but with  $\varrho_{ij}$  replaced by  $\varrho_i = (|\mathbf{r}_i - \mathbf{r}_c| - \sigma_c + \sigma_0)/\sigma_0$  and  $\sigma_c = R + \sigma_0/2$ . Here,  $R$  is the colloid radius, and  $\mathbf{r}_c$  the position of the colloid center. This interaction potential results in homeotropic anchoring of the liquid crystal molecules, normal to the particle surface.

The systems consist of 8,000-1,000,000 mesogens. A molecular dynamics program was run on a Cray T3E using a domain decomposition algorithm. The colloid particle was fixed in the center of the box. The director was constrained along the  $z$  axis.

## References

- [1] P. Poulin, H. Stark, T. C. Lubensky, and D. A. Weitz, *Science* **275**, 1770 (1997).
- [2] T. C. Lubensky, D. Petey, N. Currier, and H. Stark, *Phys. Rev. E* **57**, 610 (1998).
- [3] O. V. Kuksenok, R. W. Ruhwandl, S. V. Shiyonovskii, and E. M. Terentjev, *Phys. Rev. E* **54**, 5198 (1996).
- [4] R. W. Ruhwandl and E. M. Terentjev, *Phys. Rev. E* **56**, 5561 (1997).
- [5] H. Stark, *Euro. Phys. J. B* **10**, 311 (1999).
- [6] J. G. Gay and B. J. Berne, *J. Chem. Phys.* **74**, 3316 (1981).
- [7] S. V. Shiyonovskii and O. V. Kuksenok, *Mol. Cryst. Liq. Cryst.* **321**, 489 (1998).

## Acknowledgements

This research was supported by EPSRC. G.G. acknowledges the support of a British Council Grant; M.P.A. is grateful to the Alexander von Humboldt foundation.

## Off-center ring

Simulation results show that both the satellite and ring defects are at least metastable for  $R/\sigma_0 = 15$ : once the particular defect is realized in the system, it is stable over the timescale that is accessible to our simulations. However, the satellite defect is not stable for the smaller droplets. Indeed, we observed a rapid transition of the satellite defect to the ring defect for  $R/\sigma_0 < 10$ . Equilibrating the initial configuration with the satellite defect in the cell with droplet radius  $R/\sigma_0 = 10$ , we observed that it evolves into an off-centered ring defect: a typical nematic director map is shown in Fig. 12.

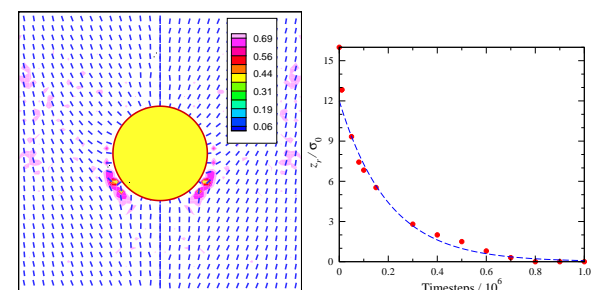


Figure 12 Director map for the off-center ring configuration. The background contour plot represents the value of the order parameter.

Figure 13 Dynamics of the transition from the satellite defect to the Saturn ring defect via an off-center ring configuration.

The ring moved slowly, evolving towards an equatorial Saturn ring configuration. Doing long runs (up to a million timesteps) we conclude that this is an intermediate state between the satellite and the Saturn ring defect. The  $z$ -coordinate of the ring, relative to the droplet center, as a function of the number of the timesteps, is shown in Fig. 13. The evolution dynamics is quite slow. Note that elastic theory also predicts the off-center ring configuration to be unstable [5], with the transition from the dipole configuration to the Saturn ring configuration occurring via this intermediate state.